 doi:10.20944/preprints202206.0200.v1

Article

Design of a Compact Energy Storage with Rotary Series Elastic Actuator for Lumbar Support Exoskeleton

Omar S. Al-Dahiree [1,2,*], Raja Ariffin Raja Ghazilla [1,*], Mohammad O. Tokhi [3], H. J. Yap[1], and Emad Abdullah Al-baadani[4]

[1] Department of Mechanical Engineering, Faculty of Engineering, University of Malaya, Kuala Lumpur, Malaysia.; (H.J.Y.) hjyap737@um.edu.my
[2] Engineering, computer, and mathematical sciences, Auckland University of Technology, Auckland, New Zealand; omarsmech@gmail.com
[3] School of Engineering, London South Bank University, London, UK; tokhim@lsbu.ac.uk
[4] Department of Electrical Engineering, Faculty of Engineering, University of Malaya, Kuala Lumpur, Malaysia; (E.A.A) mr_emad93@hotmail.com

* Correspondence: (O.S.A) omarsmech@gmail.com , (R.A.R.G.) r_ariffin@um.edu.my

Abstract: Lumbar support exoskeletons with active and passive actuators are currently the cutting-edge technology for preventing back injuries in workers while lifting heavy objects. However, many challenges still exist in both types of exoskeletons, including rigid actuators, risks of human-robot interaction, high battery consumption, bulky design, and limited assistance. In this paper, the design of a compact, lightweight energy storage device combined with rotary series elastic actuator (ES-RSEA) is proposed for use in a lumbar support exoskeleton to increase the level of assistance and exploit the human bioenergy during the two stages of the lifting task. The energy storage device takes the responsibility to store and release passive mechanical energy while RSEA provides excellent compliance and prevents injury from the human body's undesired movement. The experimental tests on the spiral spring show excellent linear characteristics (above 99%) with an actual spring stiffness of 9.96 Nm/rad. The results demonstrate that ES-RSEA can provide maximum torque assistance in the ascent phase with 66.6 Nm while generating nearly 21 Nm of spring torque during descent without turning on the DC motor. Ultimately, the proposed design can maximize the energy storage of human energy, exploit the biomechanics of lifting tasks, and reduce the burden on human effort to perform lifting tasks.

Keywords: Augmentation, exoskeleton, lifting strategy, lumbar support, SEA, series elastic actuator, spiral spring, machine design

1. Introduction

Heavy lifting and carrying, frequent trunk bending, and regular squatting are considered risk factors for lumbar spine injuries in working environments. The current trend is toward mechanization in industry and the use of mechanical aid devices during manual handling tasks. Despite these insights, when loads are within the human lifting ability range, the workers are willing to lift manually. Most of the mechanical lifting equipment is slower than human speed and is sometimes not easily accessible. Thus, to assist the worker, apply a system that can assist the waist movement in the direction of anti-gravity. Exoskeletons as on-body lifting aids facilitate robotic support while preserving human flexibility and intelligence [1]. Exoskeletons can be defined as wearable bionic devices equipped with powerful actuators at human joints that integrate human intelligence and robot power [2]. Wearable hip or trunk exoskeleton suits are necessary interventions currently being developed to help workers prevent lumbar spine injury. They can relieve back pain and avoid injuries by reducing the muscular effort or lumbar stress required for

 doi:10.20944/preprints202206.0200.v1

balancing or holding heavy objects [3,4]. Generally, the system is configured to transmit assistive torque to a wearer's torso through actuators at both hip joints.

Various lumbar support exoskeletons have been developed and commercialized for real industrial environments to support workers and prevent back injuries [5]. However, research efforts are still carried out for the development of lighter and more powerful exoskeletons for enhanced performance in terms of assistance. Depending on the nature of the assistive force or torque required, exoskeleton actuators can be classified into passive and active types. Passive lumbar support exoskeletons use viscoelastic elements such as springs and dampers to assist in lifting tasks. Several of these exoskeletons have been developed, such as WMRD [6], SPEXOR [7], BNDR [8], Laevo [9], and BackX [10]. Both WMRD and the hip joint of SPEXOR use coil springs, while BNDR employs compact torsion springs. WMRD provides a 54% reduction in back muscle activity, and SPEXOR generates an assistive torque with a16% reduction in muscle activity by utilizing flexible beams combined with coil springs. BNDR reduces the lumbar compression load without transferring the load to the joints, thus reducing the compression and sheer force of the low back by 13% and 12%, respectively. Laevo and BackX utilize gas springs to provide passive assistance to reduce lumbar muscle fatigue even though these actuators are not considered lightweight. Several passive exoskeletons use elastic bands, such as Personal Lift Assistive Device (PLAD) [11], Smart Suit Lite (SSL) [12], Wearable Assistive Device (WAD) [13], and biomechanically assistive garments[14] . PLAD adopts elastic bands to reduce 38% of the spinal muscle activity during the squat posture. Furthermore, VT/Lowe's exoskeleton [15] applies carbon fiber beams to provide higher assistive torques when compared with gas springs, reducing the peak and average of back muscle activity by 31.5% and 29.3%, respectively.

These passive exoskeletons are incapable of producing enough power and assistance to reduce muscle activity [16]. For this reason, active lumbar exoskeletons have been developed to add external energy to human motion by using a power source to activate the actuators. These exoskeleton designs comprise one or more actuators that augment the human power and help to actuate the human joints with, for example, electric motors, pneumatic artificial muscles (PAMs), hydraulic actuators, and soft actuators [17]. Some examples of exoskeletons with motor actuators are SIAT-WEXv1 [18], SIAT-WEXv2 [16], Hyundai H-WEX v1 back-support [5], Hybrid Assistive Limb (HAL) [19], ATOUN Model A, and Y [20]. SIAT-WEXv1 uses a DC motor with a harmonic drive to provide the assistive torque and a clutch to increase the battery-powered run time, while SIAT-WEXv2 uses a quasi-direct drive to assist the hip joint during a lifting task, leading to a reduction rate of EMG at lumbar erector spinae (LES) of monotonically 40% to 60%. A single actuator mounted on the back of the H-WEXv1 exoskeleton has been designed and integrated with wire drive to transfer the motion to the hip joint for lifting objects. The main muscle activities have been reached by 10% to 30%. Perhaps the best-known developed robotic suit is Cyberdyne's Hybrid Assistive Limb (HAL). The HAL for care support has enabled to reduce the magnitude of muscle force (lumbar erector spinae (LES) declined by 14%) and the onset of muscle activity (LES reduced by 4.5%) in the lower back during a repetitive lifting task [19]. Consequently, it can be seen that most of the active exoskeletons use electric motors, even though there are some examples of using pneumatic actuators (e.g., Muscle Suit [21]) or hydraulic actuators.

One of the significant problems associated with the current active actuators of exoskeletons is that they are rigid and stiff. They cannot, therefore, effectively adapt to unpredicted external impact loads or obstacles and thus produce high impedance and resistance to any dynamic behavior of human movement. To mitigate the drawbacks and safety risks of rigid actuator designs, the mechanical configuration of the elastic element with an electric motor has been proposed. This configuration provides many advantages over rigid actuators [22], such as low mechanical output impedance, back-drivability, tolerance to impact loads, high force/torque controllability, and fidelity. It has been found that only a few studies in the application of lumbar support exoskeleton adopted the configuration of the elastic element-electric motor. An example of a parallel arrangement is

 doi:10.20944/preprints202206.0200.v1

the active trunk module (Robo-Mate) [23], which incorporates a parallel-elastic actuator (PEA) to meet the torque requirements of manual handling of the object in industrial environments. It provides a significant reduction in muscular activity in the lumbar spine (around 30%). Another configuration is the series elastic actuator (SEA), where two studies are noted in the literature for lumbar support exoskeleton at hip joints. The lower back exoskeleton [24] uses four SEA units with a clutch to generate effective assistance, providing a continuous torque of approximately 40 Nm on both hip joints to actively assist both hip abduction/adduction and hip flexion/extension. H-WEXv2 [25] utilizes an SEA-based wire-driven mechanism, as reported, the muscle intensity of erector spinae and gluteus maximus are reduced by 33.0% and 41.6% in semi-squatting posture, respectively.

Lumbar support exoskeletons with active actuators demand power sources (e.g., batteries) that increase the device's overall weight and limit their operational time due to increased battery consumption during the entire cycle of the lifting task. Passive exoskeleton, on the other hand, can only provide limited assistance to users due to the physical nature of passive device components. Moreover, current studies of passive actuators for lumbar support applications do not consider the biomechanical energy conversion and management of lower limbs during the phases of lifting tasks, which involve periodic motion acceleration and deceleration. According to the different energy conversion forms, elastic energy is one form of physical-mechanical energy storage that is pollution-free, reusable, and low cost. Therefore, the exoskeleton acquires the biomechanical energy from the negative power of the lower limbs and then supports the acceleration of the lower limbs during the lifting task. Hence, the exoskeleton can assist in lifting in the absence of external force, which is a very promising idea.

Passively storing and releasing energy might be accomplished mechanically through the practical use of a mechanical spring. Since a mechanical spring system has properties similar to the human lower limb muscle-tendon unit and thus may compensate for the function of muscle tendon units partly, the spring can store and absorb the kinetic energy of the deceleration phase during the lifting task. In this case, biological energy consumption can be reduced, and lifting assistance can be accomplished. The concept of energy transfer between the human joint and exoskeleton has been investigated, such as the study of the unpowered knee exoskeleton [26] that utilizes a crossing four-bar mechanism integrated with a torsion spring to reduce the energy consumption during cycling with no additional power supply. However, in the application of lifting task exoskeleton, the hip joint's energy transfer concept has not yet been incorporated into functional designs.

Thus, to resolve the issue of exoskeleton dependence on a large power supply and at the same time save human bioenergy and increase the level of assistance, achieve the function of energy storage, conversion, and management. This paper presents the design energy storage unit integrated with a rotary series elastic actuator (ES-RSEA) for lumbar support exoskeleton application to assist the hip movement during lifting tasks by utilizing the negative work of the lower limbs. The exoskeleton mainly consists of a spring storage unit, where the flat spiral spring stores mechanical energy from the lower limb descent stage and then releases it to assist the acceleration motion. The research work presented in this paper aims to provide an alternative method to harness the kinetic energy of the human limb to assist semi-squat lifting tasks along with an active compliance actuator. The paper's main contribution is a new actuation system that utilizes the advantage of the dynamic movement of the human body during the lifting of loads to store energy and release additional output power, to enhance the function of the lifting strategy for an exoskeleton and reduce battery consumption. To the authors' knowledge, this study is the first to propose an SEA with an energy storage unit (a spiral spring) in a compact and modular design for a lumbar support exoskeleton to improve energy migration, assistance across human lower limbs, and mechanical safety.

 doi:10.20944/preprints202206.0200.v1

2. Biomechanics of Lifting Task

Load lifting is a standard energy-consuming industrial operation [27]. Low back pain and back injuries can occur as a worker lifts an object continuously, holds heavy loads in a static pose, and twists back due to a heavy load [5]. Of the various lifting techniques, the most often employed are squat, semi-squat, and stoop lifting. Each lifting technique has been stated to possess benefits and challenges based on differences in the occupational environment, as there is no single best posture technique for all situations [28]. Semi-squat lift technique may be considered a good compromise between the stoop and squat. Workers may also find this to be closer to the natural movement pattern for lifting tasks and more practical in most environments. Therefore, it is adopted to be the main technique for designing the proposed exoskeleton.

There are various kinds of energy conversions taking place during the daily tasks carried out by human beings. In the process of human movement, a significant amount of kinetic energy will be generated in the human body, reaching 200 W [29]. One of the most critical aspects is the human squat. In the squat lifting cycle, since the lower limbs sustain and bend the whole body forward, they provide substantial kinetic energy in the ascent and descent movement stages. Potential energy and kinetic energy are continuously converted within the body throughout the squat lifting phase. Consider that an additional mechanism device is utilized in the deceleration phase to absorb the kinetic energy of the lower limb and transform it into potential energy, and temporarily store it for the next acceleration phase of the limb joint. In that case, biological energy consumption can be reduced, and lifting assistance can be accomplished.

2.1. Human Musculoskeletal System

Skeletal muscle contractions, the most significant tissue function in the body, contribute to 40 percent of the body weight, reinforcing the body's different movements and breathing behavior. Multiple body joint motions are performed by the bone and joint cooperating through the contraction and release of skeletal muscle. The muscle contraction occurs due to stimulation of the motor neuron by receiving an electrical signal caused by either artificial electricity or the body's own response. Muscle contraction operates and functions on the skeletal bars connected to it to provide muscular tension to relieve outward resistance or pressure, rotating around the joints. Moreover, muscles often include various contraction activities depending on the different movement phases within the lower limb activities [30].

The muscle drives the movement of the joint. Through the tendon attached to the bone, the muscle transmits the driving torque and force of the joint to the human body. The lower limb muscles contract, stretching the joints and generating torque on them during squat lifting. The mechanical work of joint movement describes the transfer of energy from one part of the body to another [30,31]. During squat lifting tasks, muscles can generate both positive and negative mechanical work. Muscles convert the metabolic energy of the human body into mechanical energy when doing positive work.

The hip joint can be considered as a ball and socket, which is enclosed with strong and steady muscles, allowing a wide range of movements in multiple physical planes and still being remarkably stable [32]. The hip's geometry allows rotational motion in every direction to maintain appropriate stability, requiring a high number of muscle controls originating from a broad surface area. There are 22 muscles in the hip joint, operating to stabilize it and generate the force needed for the hip movements. The hip's muscular anatomy is classified into adductor group muscles; inner and outer hip muscles [33]. In terms of human anatomy, the Gluteus Maximus, situated on both hips, is the primary muscle involved in the waist and hip movement, as seen in Figure 1 [5,32]. These two muscles operate as one synchronized muscle during waist flexion and extension due to the rotation orientation of both hip joints being the same during waist flexion and extension. This implies that an actuator on each hip joint might aid in waist motions. The muscle activity of thigh muscles is of interest when performing a squatting exercise [34]. Notably, the quadriceps show more significant muscle activity than the hamstrings during the complete

Preprints (www.preprints.org) | NOT PEER-REVIEWED | Posted: 14 June 2022 doi:10.20944/preprints202206.0200.v1

ascent phase [27]. The focus is to relieve muscle groups of the burden of working concentrically and eccentrically to control the motion of the knee joint.

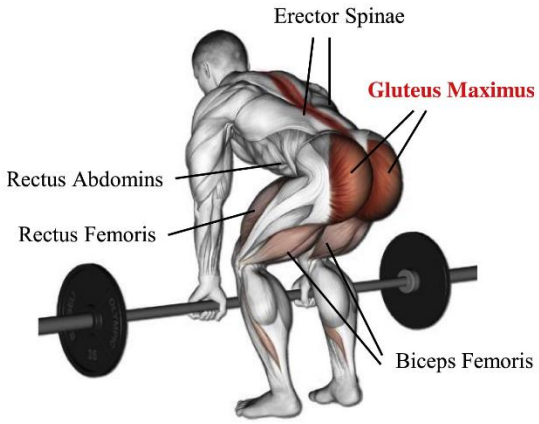

Figure 1. Anatomical analysis of waist motion during a squat lifting task.

2.2. Biomechanical Analysis of Human Body During A Lifting Task

Biomechanical techniques have helped understanding of the loading conditions that cause lower back pain and the development of techniques for prevention of musculoskeletal disorders in workers through force assistance for the lumbar spine during lifting tasks. The biomechanical study of the lumbar spine in postures related to lifting tasks is covered in this section. The scientific literature suggests approaches for estimating load and moment on lumbar spines based on either static and dynamic analyses that lead to a biomechanical model for loading the spine or via experimental measurements for the muscle activity during the lifting [35].

The study here has adopted human kinematics and kinetics data from reference [36] to determine the moment, power, and load assistance of the lumbar spine during the lifting task. Biomechanical data during squats were collected and analyzed by using a motion capture system, force plate sensors, and EMG sensors. During the lowering or lifting of the load via extension action, the peak requirements were recorded. Therefore, kinematics analysis is used to investigate the system's motion. The torque and power required to lift a 15 kg load are 110 Nm and 310 W, respectively with a speed of 2.6 rad/s for the hip joint. However, the actuator's targeted assistance torque is almost 50% of the required torque to lift the load between 5 kg and 25 kg. Biomechanical data were used to verify the design of wearable assistive devices. In addition, the actuation's required characteristics to be implemented on each joint were determined using joint torque data. Since the joint torque distribution varies within the semi-squat tasks. It is popular to design the actuators based on the peak torque values [37].

The kinematic; degree of freedom (DOF), kinetic (joint torques), and range of motion (ROM) characteristics of lower limb biomechanics represent movements' static characteristics. However, the lifting task is dynamic and is characterized by joint rotational speed and the frequency bandwidth of the movements [37]. The frequency bandwidth of the hip joint's human motion ranges from 4 Hz to 8 Hz [38]. The actuator's bandwidth should at least fulfill the frequency elements of human motion in order to respond rapidly to the control signal. Moreover, the actuators are designed analogously to the human muscles to mimic the human muscles' function during lifting tasks [39]. The design requirements that depend on biomechanical data are summarized in Table 1.

.

Preprints (www.preprints.org) | NOT PEER-REVIEWED | Posted: 14 June 2022 doi:10.20944/preprints202206.0200.v1

Table 1. Actuator design requirements

Parameter	Value
Range of motion	110° to -15°
Maximum joint velocity	2.6 Rad/s
Maximum joint torque	110 Nm
Maximum joint power	310 W
Bandwidth range of joint	4-8 Hz
Torsional spring stiffness	450 Nm/rad
Spiral spring stiffness	10 Nm/rad

2.3. Actuator Design Considerations

Figure 2 shows the conceptual design of ES-RSEA. This compliant actuator of a soft trunk-hip exoskeleton enables the design of a portable and lightweight system with higher torque delivery and further lumbar assistance while maintaining high compliance, safe human-robot interaction, and faster adaptation to human movements. The actuation unit ES-RESA includes a modular and a compact rotary SEA integrated with an energy storage unit. The RSEA provides mechanical compliance with a high torque-to-weight ratio at the interface between the exoskeleton and the user. On the other hand, the energy storage unit is proposed to provide additional torque based on the biomechanical energy conversion of the human lifting cycle. The uniqueness of the design concept combines a precise mechanical design of assistance timing with high robustness and repeatability.

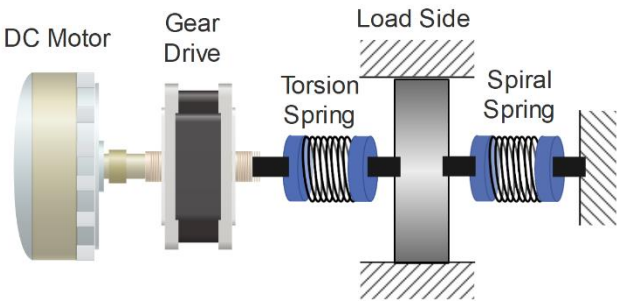

Figure 2. Conceptual design of ES-RSEA

The central concept for designing the lower limb exoskeleton is according to the anthropometric factors of the human body. The interaction between the human body and the exoskeleton is determined by whether the design is anthropomorphic or non-anthropomorphic [40]. Moreover, the lumbar support exoskeleton design is based on the Malaysian population, and so the anthropometric data for Malaysian workers is collected according to reference [41]. Therefore, the lumbar support exoskeleton is considered anthropomorphic, meaning that the pelvis and thigh components of the exoskeleton move similarly to their human equivalents. Figure 3 gives an overall perspective and a detailed view of the lumbar support exoskeleton worn on the human body.

Preprints (www.preprints.org) | NOT PEER-REVIEWED | Posted: 14 June 2022 doi:10.20944/preprints202206.0200.v1

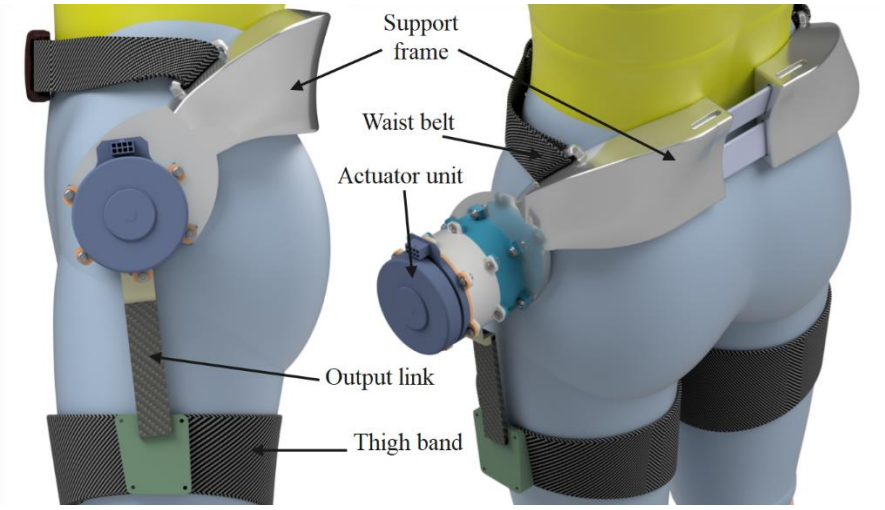

Figure 3. Soft trunk-hip exoskeleton schematic

The range of motion of the human joints forms a critical biomechanical factor of an exoskeleton. By analyzing human joints' movements during the lifting tasks, the joints' comfort angles have been defined, as shown in Figure 3, to prevent any pain or even danger to humans during the lifting postures [35]. Moreover, the ROM of the hip joint is sufficient to provide lifting tasks. Flexion/extension, adduction/abduction, and internal/external rotations are the three rotational DOF of the hip joint [37]. The hip flexion/extension is the active actuated DOF of the proposed exoskeleton, whereas the other two DOF are passive.

Exoskeleton actuator design considerations also include a high output power-to-weight ratio as well as characteristics such as high efficiency and bandwidth, low inertia, and fast response [42]. One of the critical design factors for the SEA is the value of torsion spring stiffness, which characterizes the performance and features of the SEA. The torque measurement resolution is also influenced by the spring stiffness [43]. Thus, a suitable stiffness value needs to be chosen to trade-off between large torque bandwidth and high compliance. The literature analysis on optimum stiffness for SEA in wearable robotics applications has adopted different stiffness values ranging from 100 to 1500 Nm/rad [44-46]. These optimum stiffness values have been estimated by theoretical analyses or even by simulation studies [43], based on a trade-off between the various design criteria of SEA and the DC motor drive specification. Moreover, in this study, the proposed ES-RSEA has a low stiffness (approximately 450 N·m/rad) to improve compliance in the human-robot interaction with satisfied frequency bandwidth.

The novel part of ES-RSEA is the energy storage device. Since the spiral spring is the functional core of this device, the amount of potential energy relies mainly on the spring stiffness value. Typically, the spiral spring stiffness value K is determined carefully to ensure that the stiffness is not too rigid; otherwise, it causes over-resistance against human movement or even discomfort. Moreover, the stiffness should be softer to ensure that the spring will not adversely impact the DC motor performance during the ascent phase of the lifting task. Therefore, the spiral spring designed for lumbar support exoskeleton required spring constant K = 10 Nm/rad, maximum deflection θ where spring can reach 120 degrees, and maximum spring torque T_{max} of 20.94 Nm.

3. Mechanical Structure Design and Working Principle

The biomechanical principles of human lower limbs were adopted to design a lumbar support exoskeleton with a storage technique. The human squat lift reveals that in the cycle of lower limb descent and ascent, gravity energy is related to lumbar descent; the human body's weight causes a human hip joint to exert negative work. Consider that an additional mechanism device is utilized in the deceleration phase to absorb the kinetic energy of the lower limb and transform it into potential energy, and temporarily store it

Preprints (www.preprints.org) | NOT PEER-REVIEWED | Posted: 14 June 2022 doi:10.20944/preprints202206.0200.v1

for the next acceleration phase of the limb joint. In that case, it may even strengthen the human body's energy performance.

The lumbar support exoskeleton consists of three parts: the energy storage element, the series elastic actuator, and a flexible wearable structure. The exoskeleton's support frame is placed around the human centroid at the human waist to reduce the extra metabolic potential for the wearer, as shown in Figure 3. Simultaneously, the output link of the actuation system is attached to the upper part of the thigh. The actuation system, located on the hip joint, is integrated with the energy storage and the series elastic actuator. Since the spiral spring is selected as the core for the energy storage unit, the spiral spring design can maximize the spring features to extract as much potential energy as possible without ignoring the human comfort factor. Figure 3 presents the overall view of the lumbar support exoskeleton worn on a human body along with the designed actuator and a detailed view of its structure.

3.1. Mechanical Design of ES-RSEA

3.1.1. Configuration

The conventional SEA combines a motor, a transmission drive, a spring, and an output load so that the spring can directly sense the force from the output load [47]. This configuration has been adopted in many SEA designs since the first SEA was proposed. However, the proposed ES-RSEA actuator is designed with a modified version of the conventional configuration by integrating the spiral spring into the actuator's second spring. On the end of the spiral spring is attached to the output load, and the other end is fixed to the ground. The ES-RSEA configuration is illustrated in Figure 4, where the spiral spring is utilized to store and release energy, and the torsional spring is used as a compliant element. Moreover, the motor stator is fixed to the ground to efficiently transmit the torque. The gear drive amplifies the torque, so the spring's deformation can transmit the output torque. The actuator's output torque can be calculated depending on the spring deformation measurements [48]. Therefore, the spring deformation must be measured by two encoders: the motor angle and the load side angle.

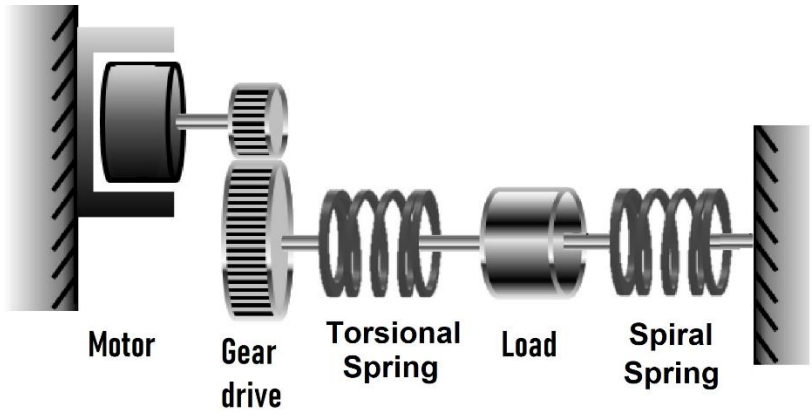

Figure 4. ES-RSEA configuration

3.1.2. Mechanical Components

Considering the requirements mentioned for the actuation system, the ES-RSEA actuator was selected accordingly. The actuator is driven by a flat DC brushless motor (EC90, 24 V, 160 W, Maxon Motor, Sachseln, Switzerland) embedded with a MILE encoder (1024 Cpt). A very compact design is made possible by the DC motor in conjunction with a 100:1 Harmonic Drive (CSD-25-100-2A-GR, Harmonic Drive®, Limburg, Germany). The Harmonic Drive is connected to the custom-made planner torsional spring, which is attached to the output link-circular disc. The torque is transmitted to the hip joint through a circular disc with an output link connected to the thigh by a bandage and baffle to the human leg. An RMB14 angular magnetic encoder (absolute-12 bit-RLS) is mounted on the

Preprints (www.preprints.org) | NOT PEER-REVIEWED | Posted: 14 June 2022 doi:10.20944/preprints202206.0200.v1

ground, while its magnet is placed on the axis output link-circular disc to measure the actual output angle. The encoder's cable is passed through a small hole drilled into the inner cylinder to protect the cables from any damage, as shown in Figure 5. A custom-made spiral spring is connected to the output link-circular disc on one side, and the other side is fixed to the actuator's case cover. Finally, the cover case of the actuator consists of two main cylindrical parts with two connecting flanges. These parts are assembled by a few bolts and nuts, which enable portability and compatibility for the proposed actuation system. The cover case with a deep sky-blue color has been designed in shape to provide mechanical brakes for the output link within the designed working motion range for the hip joint during squatting. This mechanical brake will protect the human from any motion that exceeds the human safety range of hip movements.

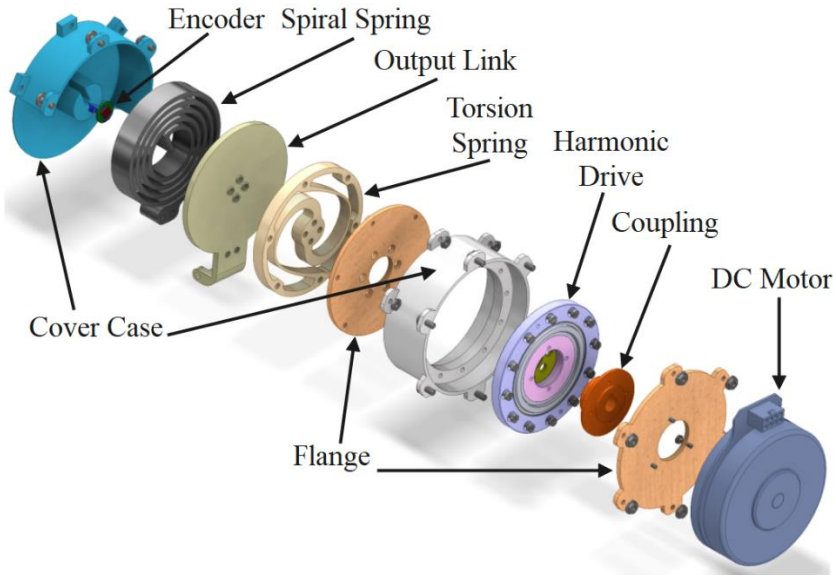

Figure 5. Assembly parts of ES-RSEA

The selected parameters of the ES-RSEA actuator are shown in Table 2. The torsional and spiral springs were designed and optimized to reduce weight and size while maintaining the required spring stiffness and spring deformation. The torsional spring was designed and optimized using the finite element method (FEM), Ansys Workbench 15.0 software, and CAD models were obtained using Autodesk Inventor, as shown in Figure 6. The maximum output torque of 45.7 Nm and the 450 Nm/rad stiffness of the torsional spring were considered desirable values of the actuator design based on actuator design considerations mentioned in section 2.3. Furthermore, the spiral spring was designed based on the fundamental spring design equations. Then spring design parameters were optimized to fulfill the purpose of the energy storage device in the ES-RSEA design, as illustrated further in the next section.

Table 2. Main features of the ES-RSEA

Parameter	Value
Max. Continuous torque of DC	0.457 Nm
Gear reduction	100
Nominal joint speed	27 rpm
Torsional spring stiffness	450 Nm/rad
Spiral spring stiffness	10 Nm/rad
Maximum diameter	105.6 mm
Radial length of the actuator	93 mm

Preprints (www.preprints.org) | NOT PEER-REVIEWED | Posted: 14 June 2022 doi:10.20944/preprints202206.0200.v1

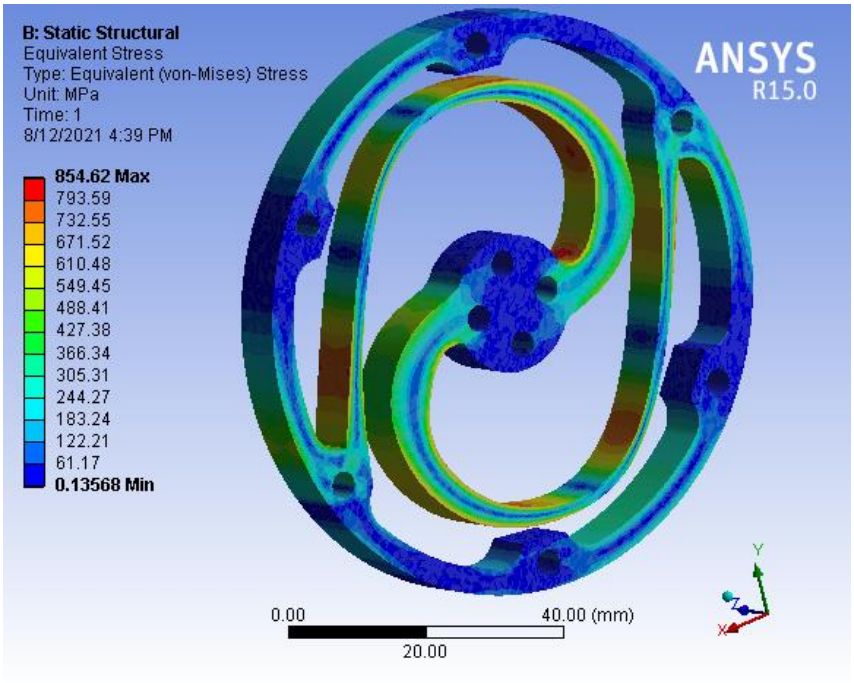

Figure 6. FEM-design for planner torsion spring

Figure 7 illustrates the cross-section of the ES-RSEA actuator. Since all the actuator parts are assembled in a compact design, the radial length of the actuator is 93 mm. The ES-RSEA actuator is mounted on the waist of the human body, particularly on the hip joint. The cover case in deep sky-blue is fixed to the robotic structure by bolts and nuts, as shown in Figure 7.

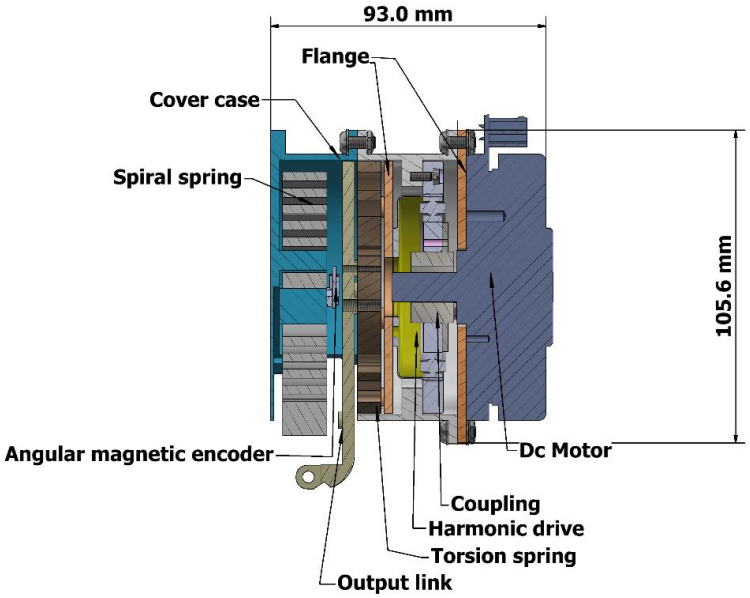

Figure 7. Cross-section of ES-RSEA

3.2. Mechanical Design of Energy Storage Device (ES)

The passive elastic element used for the energy storage device is the spiral spring. Among other types of spring, the spiral spring has excellent features for storing and releasing energy for an extensive range of deformation or angular position. Since the range of hip joint motion during lifting demands is around 120 degrees, the spiral spring would be the most suitable spring for this role. Because of its stiffness, a spiral spring will always

Preprints (www.preprints.org) | NOT PEER-REVIEWED | Posted: 14 June 2022 doi:10.20944/preprints202206.0200.v1

try to return to its original shape; it can generate the opposite torque to gravity, resulting in the minimum torque required for the hip joint. The arbor end of the spiral spring is fixed, and the torque is applied at the spring's outer radial. The torque applied bends the elastic deformation on the spiral spring strip, causing the spiral spring to rotate around its axis, storing and releasing elastic energy. It is designed to absorb and store the biomechanical energy distributed at the hip joints during the descent phase of a squatting cycle and then release it in the ascent phase. The energy stored is released from the outer end, transmitting to the thigh part by output link of actuation attached to the outer end of the spring. This passive element generates an energy-free system because no external power source is involved in the motion.

3.2.1. Design Fundamentals of The Spiral Spring

Spiral springs are the most suitable storage elements for electromechanical actuation configurations to preserve the high potential energy intrinsic to the human hip movement. The spring design is usually made from a flat rectangular strip of metal raw and wraps towards the outside of the mounting spiral spring. The torques are applied tangent to the outer ring of the spring while the inner arbor is fixed, and the angular variation between these extremities can determine the spring compliance. Additionally, springs could be coiled with a pitch P, the radial gap between coils, preventing coil interaction during spring compression. Friction losses do not exist since the coils are usually not in contact with one another. Spiral springs, as a result, have a linear torque-deflection relationship. However, since stocks of spiral springs are rarely available, they are usually manufactured to customized requirements [49].

The length L, width b, pitch P, and arm thickness t of the rectangular wound stripe are required for manufacturing spiral springs. The spiral spring design equations are taken from the handbook of spring design [50]. The geometry of a spiral spring is illustrated in Figure 8.

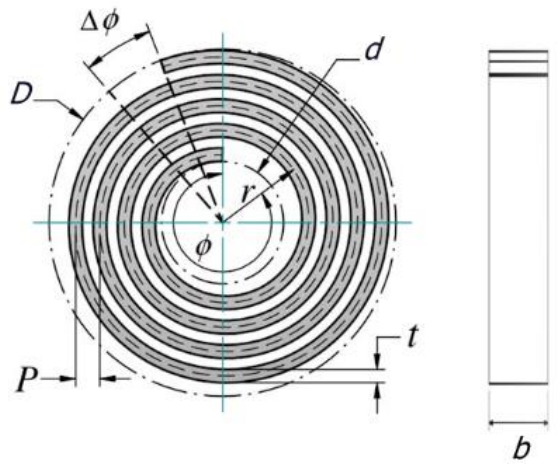

Figure 8. Schematic of a spiral spring

The maximum allowed stress, σ, which is not higher than the material's cyclic fatigue strength, can be obtained from the deflecting beam formula:

$$\sigma = \frac{6\,T_{max}}{b\,t^2} \tag{1}$$

The maximum spring torque, T_{max} is related to maximum angular deflection θ and spring stiffness K. Hooke's law describes torque exerted by a spring being deformed, which is defined by $T_{max} = K\,\theta$.

Also, the length of strip material is computed from:

$$L = \frac{E\,b\,t^3}{12\,K} \tag{2}$$

Preprints (www.preprints.org) | NOT PEER-REVIEWED | Posted: 14 June 2022 doi:10.20944/preprints202206.0200.v1

which depends on a cross-section of the strip, the material's elastic modulus E, and the stiffness value of spring K.

While the arbor diameter d is usually defined first, the minimum allowed outer diameter D is studied to prevent a tight warp-up spring on the arbor before achieving the desired deflection, which can be calculated as:

$$D = \frac{2\,L}{\pi\left(\frac{\sqrt{d^2 + 1.27\,L\,t} - d}{2\,t} - \theta\right)} \tag{3}$$

For the spring geometry design, the spiral arm shape is defined based on the Archimedean spiral and is characterized in polar coordinates (r, ϕ) described by:

$$r = a + b\,\emptyset \tag{4}$$

$$a = \frac{\left(\frac{D}{2} - \frac{d}{2}\right)}{\emptyset_{total}} = \frac{P}{2\,\pi} \tag{5}$$

$$b = \frac{d}{2} \tag{6}$$

The spiral angle ϕ and radial distance r at a given angle are the factors that shape the spiral arm, while the coefficients a and b are respectively calculated via equations (5) and (6) where $\emptyset_{total}$ denotes the spring's total wrap angle.

Also, the spiral arc length L_{arc} equals the length of the strip in equation (2), computed as

$$L_{arc} = \int_0^{\emptyset_{total}} r\,d\,\emptyset = \emptyset_{total}\left(a + \frac{b}{2}\,\emptyset_{total}\right) \tag{7}$$

The type of designed spring is called brush spring. These types of spring are often deflected less than 360 degrees and are generally subjected to the following design requirements.

Length-to thickness ratio L/t should be between 200 and 1000.

Width-to-thickness ratio b/t should be within a range of 3:1 to 15:1.

The allowable stress should not exceed 1000 MPa.

Grade 304 stainless steel was selected as the spring material due to its low-cost material and ease to manufacture with excellent yield strength. Design for manufacturing (DFM) is considered an essential factor for designing spiral springs. In this study, the cutting machine technology that used water jet cutting exposes spiral spring geometry dimensions to several design constraints. The material 304 stainless steel plate is widely available with a specific width range of 8, 10, 12, and 15 mm. The waterjet cutting stream's width (nozzle size) determines the minimum value of (P-t) to 2 mm. The pitch P is the space between the spiral arms that a waterjet cutting stream can efficiently cut. It also enables the coils to wind freely until the specified load is reached. In addition, the arm thickness t should not be less than 2.5 mm to avoid any material failure and increase bearing stress for torque load.

Furthermore, the spiral spring element is deeply integrated with the proposed actuation layout, so the spiral spring's design mechanism should be compatible with actuator parts. The arbor diameter d was selected as 30 mm, grounded in the actuator's case, and the maximum outside diameter D was chosen at 80 mm, attached to the actuator's output link.

3.2.2. Design of Spiral Spring

The design procedure to accomplish a suitable and optimal spring width b, arm thickness t, and pitch P depends on the design requirements and allowable range of spring parameters mentioned in the previous section. This design method can lead to an efficient spiral spring design for a proposed energy storage device. The first design step is to find all possible range values of t and P with a given thickness b, which would not exceed the allowable stress of the material. Figure 9 shows the spring parameters thus required, where each point in the painted surface represents a feasible range of spring parameters

Preprints (www.preprints.org) | NOT PEER-REVIEWED | Posted: 14 June 2022 doi:10.20944/preprints202206.0200.v1

(t and P with b). Secondly, since the minimum allowable value for (P-t) is 2 mm, it is rational to remove all points from the painted surface that do not meet this condition. The resulting points are shown on the painted surface in Figure 9 with dark color.

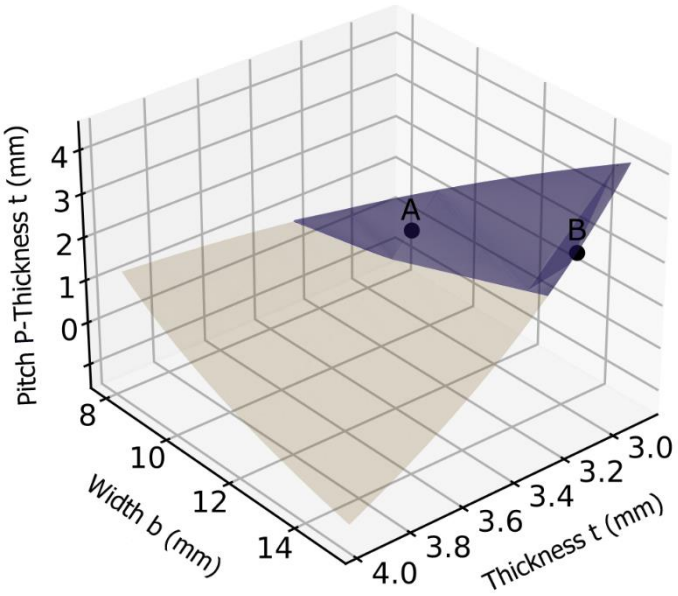

Figure 9. Parameter design for spring

The fatigue strength of wide and thin springs is higher, but at the cost of increased total volume and weight of the spring. It appears from the dark colored surface in Figure 9 that the feasible range of material width b is narrowed, whether 15 or 12. Thus, the optimum design parameters at width 12 and 15 are denoted in Figure 9 as A and B, respectively. Table 3 shows the spring design parameters of the optimum design of A and B. As a compromise, a spring, denoted as B, with t= 3.1 mm, b=15 mm, and P-t=2.7 mm, was chosen. It was considered short enough to fit within the compact actuator while maintaining good fatigue strength. Its maximum stress σ is 871 MPa, which is much lower than the allowable material stress. The CAD for the designed spiral spring based on the obtained geometry design is shown in Figure 10

Table 3. Optimum spring parameters

Parameter	A	B
P-t	2.45	2.7
σ	938	871
b	12	15
t	3.34	3.1
b/t	3.6	4.84
L/t	223	240

Preprints (www.preprints.org) | NOT PEER-REVIEWED | Posted: 14 June 2022 doi:10.20944/preprints202206.0200.v1

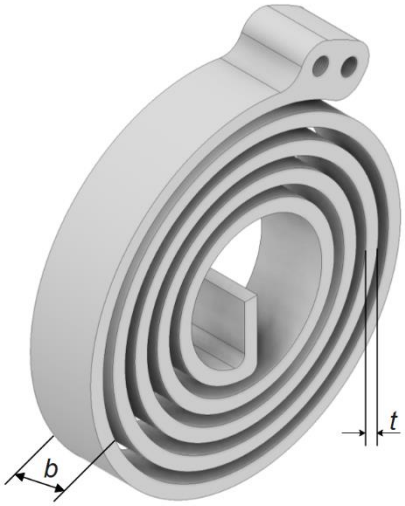

Figure 10. CAD for designed spiral spring

3.3. Working Principle

The mechanical structure of the energy storage-rotary series elastic actuator (ES-RSEA) is shown in Figure 5. The assistance torque of ES-RSEA is generated by the DC motor and energy storage device. The torque generated by the energy storage device can be in two phases. In the descent phase, the assistance torque is generated by the compression of the spiral spring. The spiral spring is fixed from the inner end to the cover case while the outer end rotates synchronously with the attached leg through the output link. The proposed design of the energy storage device implemented with SEA enables the spiral spring to rotate based on the motion range of the hip joint. On the other hand, the assistance torque of the ascent phase is generated by the release of the stored energy in the spiral spring. The direction of this assistance torque will be the opposite of the first phase. In the ascent phase, the torque assistance of the DC motor is combined with the released torque of the spiral spring. The DC motor generates continuous torque due to the torque reference commend. Subsequently, the harmonic drive reduces the speed (the speed output is less than the speed input). Since torque output will be the inverse of the speed function, output torque will increase due to the drive ratio of harmonic drive (drive reduction = 100). After the harmonic drive, the torque is transmitted to the output link through a torsion spring. The torsion spring, as a compliant element, will provide stiffness and flexibility along with torque transmission to the output link. Finally, the output link is driven by the DC motor and associated with the movement of the hip angle. At the same time, the release torque of the storage device will rotate the output link in the same direction. Therefore, the output assistance torque in this stage is a combination of the two output torques.

4. Energy Flow and Semi-Squat Lifting Strategy

The energy storage device largely depends on the human body's dynamic movement. During the squat lifting process, the muscles absorb human bioenergy dissipated at the biological hip joint. Nevertheless, while the activation muscles need to exert negative work to stand against the hip joint movement, a proportion of these muscle functions can be substituted, and the consumption of energy in muscles might be reduced by transferring the kinetic energy of hip joints to the storage element of the exoskeleton's actuation system, where it is transformed to elastic potential energy. If, subsequently, the hip joint needs to be driven by positive work from muscles, the exoskeleton's storage element, particularly the spiral spring, can release a portion of the energy stored and transformed it to kinetic energy to assist the hip joint movement. This conversion of energy assists the muscles and the human body in reducing energy consumption. However, elastic energy,

Preprints (www.preprints.org) | NOT PEER-REVIEWED | Posted: 14 June 2022 doi:10.20944/preprints202206.0200.v1

which has relatively inexpensive, renewable, and emission-free properties, is among physical-mechanical energy storage. Also, one of the proposed alternatives to subdue the power constraints is elastic energy, which provide a sustainable source of energy to power the dynamic movement of the exoskeleton [30].

Since the human body governs the hip joint to consume much negative work during the squat lift in the lowering phase, especially when lifting loads, pathological changes and shrinkage will occur in the hip joint. A fraction of this energy may be captured by the exoskeleton through the energy storage device. The stored energy can be released for assistance once the hip joint requires positive work during the lifting phase. Furthermore, the power fluctuation is varied significantly and synchronously between positive and negative work during the phases of semi-squat lifting, making energy storage and release for the hip joint sufficient. Accordingly, the hip joint needs more positive power and may also exert negative power steadily in the squat lifting cycle [30].

Based on the analysis of the human body's energy distribution and biomechanics during lifting tasks, the storage element integrated into the actuation system is installed at the human body's hip joint. First and foremost, during the lifting tasks, the hip joint has the most extensive range of joint motion . For this reason, the hip joint has been chosen rather than the knee and ankle joints, and the extensive range of hip joint motion indicates that it can provide sufficient and high energy storage. Consequently, the actuation mechanism does not interact but has the most wearable daily activity for workers during the manual handling tasks.

4.1. Lifting Strategy for Descent and The Ascent Phase

The power and torque assistance for the proposed lumbar support exoskeleton depend mainly on the delivery of assistance from the actuation system; SEA is integrated with the energy storage element. In other words, the performance and operation setting of the spiral spring and DC motor determine the lifting strategy during the descent phase, and ascent phase of the squat cycle, as shown in Figure 11 with the working principle of the storage device during each phase. Each phase adopts a different function strategy between active and passive actuation of the DC motor and spiral spring, respectively. Moreover, the proposed lifting strategy provides several benefits related to assistance percentage, battery consumption for motors, and biomechanics employment.

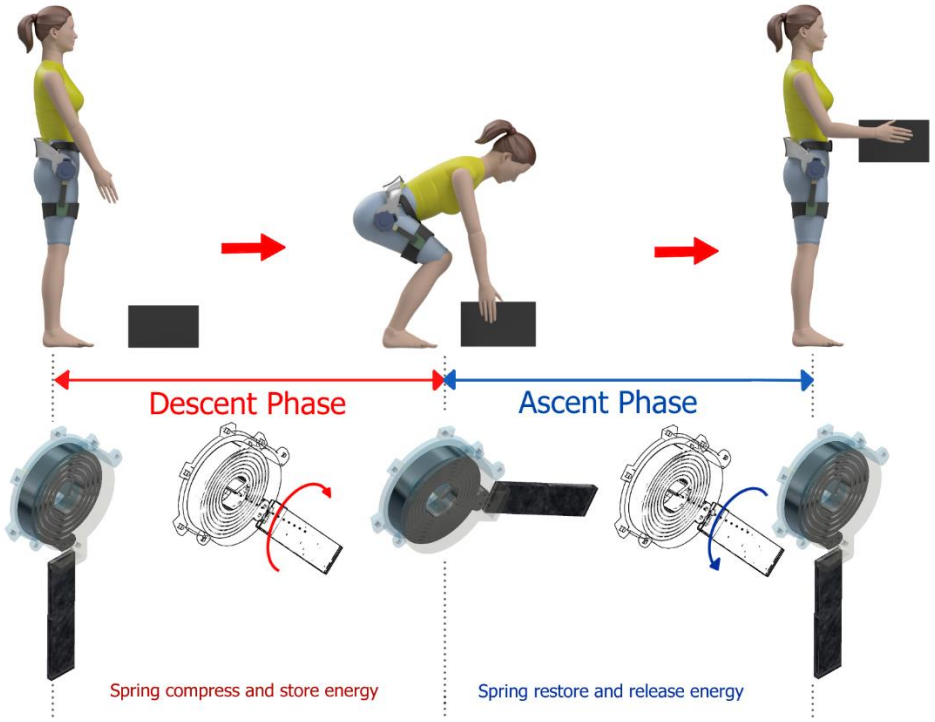

Preprints (www.preprints.org) | NOT PEER-REVIEWED | Posted: 14 June 2022 doi:10.20944/preprints202206.0200.v1

Figure 11. Working principle of the energy storage device

Firstly, the descent phase is the first step of squat when needed to pick up a load from the ground. During this phase, the type of assistance required is to hold and resist the inertia of a human body against its movement. Therefore, the spiral spring is employed to store the energy produced by human weight impact, applying torsional torque on the spiral spring till it reaches a fully compressed state at the end of the phase. The spiral spring serves as a passive device and provides resistance torque opposite to human gravity. Since the resistance torque principally depends on the value of the spring stiffness, the stiffness is chosen to provide sufficient resistance but not to exceed the human comfort limits. In addition, the spiral spring storage and compliance of the SEA prevent the adverse impact of human gravity on the DC motor. Furthermore, the DC motor is not powered during the whole descent phase. Thus, there is no battery consumption during the descent phase, which lengthens the overall battery life of the exoskeleton device.

The ascent phase of lifting squat demands significant assistance for lifting the loads. Only in this phase does the human receives two assistance sources synchronously, namely the output torque of SEA and the released energy of the spiral spring. The DC motor is powered and runs in the same direction as human movement to exert positive work. Simultaneously, the spiral spring starts to release its energy and torque stored during the descent phase. Since the released torque of the spiral spring and the SEA output torque are oriented toward the same direction, there is no energy loss between the output of the SEA and the spring. Consequently, the two assistance torques collaborate with one another. Thus, the proposed actuation mechanism would provide a higher level of assistance compared to sole DC motor.

3.2. Energy Storage and Delivery

Elastic potential energy is energy stored as a result of applying a torque to deform spiral spring. The proposed spiral spring can store the energy until the angular deformation reach its designed limit then spring back to its original shape, exerting work in each process. This exerted work can be used for driving and rotating the hip joint and generates torque assistance. Spiral spring designed to store elastic potential energy will typically depend on the stiffness value and maximum angular deformation. The spiral spring's stiffness curve, also known as the characteristic curve, defines the relationship between the torque T and angular position θ. A designed spiral spring's primary behavior is the linear characteristic curve since the spring is coiled firmly and no energy is lost in an ideal spring, as illustrated in Figure 12. The torque-angular position relation is formed on Hooke's law formula which is defined by $T = K\theta$. In addition, the elastic energy storage can be calculated from the work done by the spring, representing the area under the torque-angular deformation curve in **Error! Reference source not found.**, is given by $E_{store} = \frac{1}{2} T\theta$, or $E_{store} = \frac{1}{2} K\theta^2$ [51].

Preprints (www.preprints.org) | NOT PEER-REVIEWED | Posted: 14 June 2022 doi:10.20944/preprints202206.0200.v1

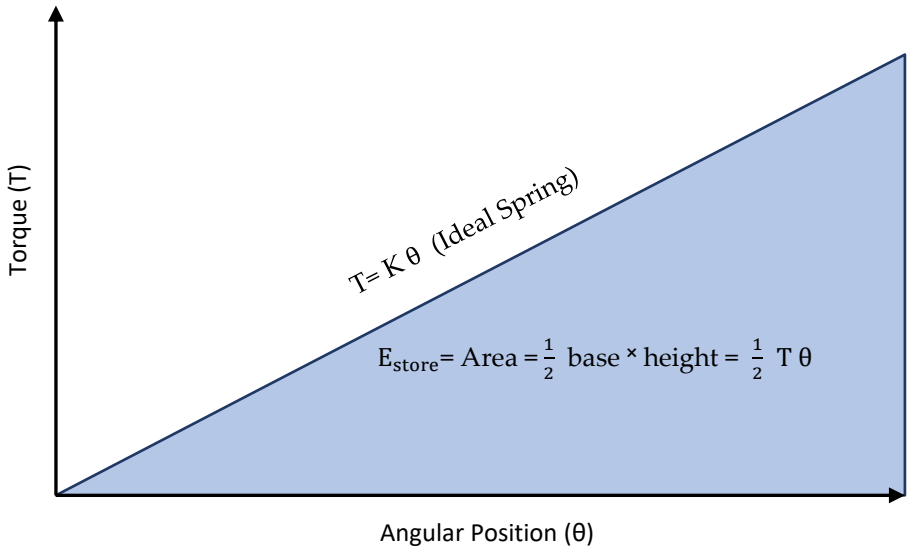

Figure 12. Relationship between the torque and angular position

The variation in the human biomechanical power of the hip joint during semi-squat lifting besides using ES-RSEA is illustrated in Figure 12. It shows an overall trend of hip biomechanical power over time, based on lowering and lifting scenarios. During the lifting cycle, the lower limb muscles performing on the hip joint generate significant negative and positive work, using a substantial amount of biomechanical energy. The lower limb muscles acting on the hip joint produce much negative and positive work during the lifting task, which thus consumes a large amount of biomechanical energy. In the descent phase, the muscles around the hip joint mainly produce negative work for deceleration, representing areas A and B in Figure 12. However, in the ascent phase, the positive work is generated to accelerate the hip joint and reduce the impact of the gravity, considering areas C, D, and E in Figure 12.

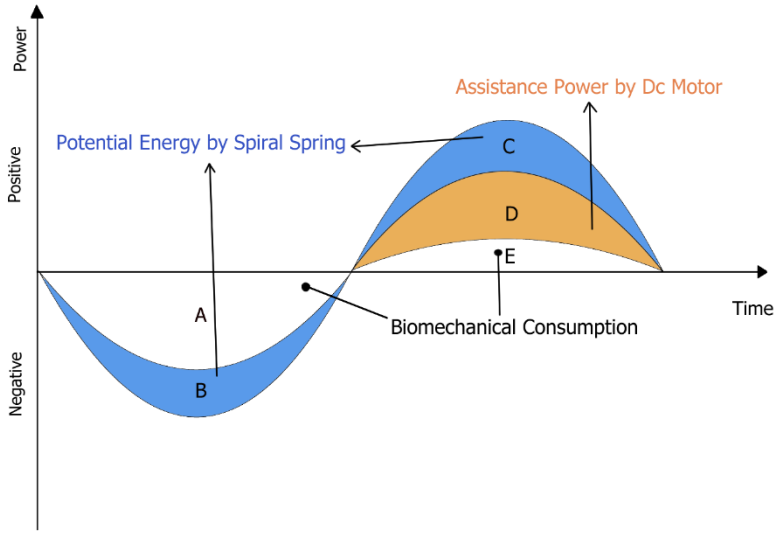

Figure 13. Theoretical description of variation in human biomechanical power using ES-RSEA.

The biomechanical energy and hip joint torque will be redistributed while the human body performs a lifting task with the energy storage device. In the descent phase, the hip movement rotates the energy storage device; the spiral spring generates resistive torque to support hip joint deceleration. The lower limb muscles are meant to execute this role of deceleration fully; nevertheless, the spiral spring performs the same job and decreases the

Preprints (www.preprints.org) | NOT PEER-REVIEWED | Posted: 14 June 2022 doi:10.20944/preprints202206.0200.v1

hip joint's negative effort. The spiral spring stores kinetic energy, as shown in Figure 12 (area B). The next ascent phase begins after that. Although the hip muscles must accelerate the hip joint, the spiral spring's potential energy is now directed to mechanical motion or torque to support the hip muscle (Area C). At the same time, the DC motor of SEA generates assistive power Figure 12 (area D). Consequently, during this phase, the positive work of the hip joint is minimized. The hip joint's biomechanical work is redistributed with the aid of the merged energy storage from SEA, with the overall metabolic energy diminished, as described in Figure 12 (area E).

The theoretical torque requirement profile of the human body during the lifting task is shown in Figure 14. During the first phase, the torque resistance is generated by a spiral spring to assist the hip joint (area A). The torque required for the hip joint is reduced (area C). Later, the ascent phase experiences significant assistive torque through a combination of the assistance torque of the DC motor and the released torque of the spiral spring, as shown in areas A and B. As a result, the required torque profile over the entire period is significantly reduced. Furthermore, the hip muscle force also reduces, empowering the user to lift the load.

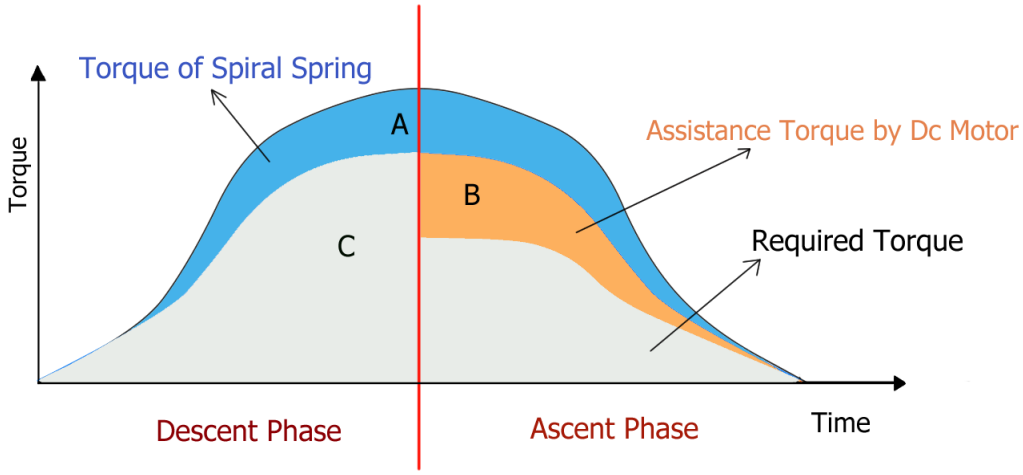

Figure 14. Theoretical illustration of the change in torque requirement of a human body when using ES-RSEA.

5. Manufacture and Experimental Setup of The Energy Storage Device

This section presents a manufacturing and experimental setup of the energy storage device as part of the proposed design in ES-RSEA for the lumbar support exoskeleton. The spiral spring is the core part of the energy storage device. The spiral spring prototype was tested and evaluated for its energy storage characteristics to evaluate the exoskeleton's effect on accurate joint assistance.

5.1. Manufacturing of The Spiral Spring Prototype

The optimized geometry design of the spiral spring has been achieved based on the theoretical framework of the spiral spring, as shown Figure 10. In addition, design for manufacturing (DFM) considerations have been conducted in the early stages of the spring design, which provides feedback to avoid any challenges or faults during the manufacturing of the final prototype. Since the waterjet cutting process can cut irregular, shaped curves and internal holes with good edge quality and exceptional precision [52], the waterjet cutting machine was selected to manufacture the spring prototype over many manufacturing processes. The available waterjet cutting machine in the local market (Malaysia) has features with a cutting accuracy of ±0.1 mm, and the nozzle's diameter (stream size) reaches up to 2 mm. Accordingly, the limitations of the used waterjet machine have been considered in the early design stage. Finally, the spiral spring prototype was manufactured from 15 mm steel plate with 304 stainless steel material, as shown in Figure 15.

Preprints (www.preprints.org) | NOT PEER-REVIEWED | Posted: 14 June 2022 doi:10.20944/preprints202206.0200.v1

Figure 15. Manufactured spiral spring

5.2. Experimental Protocol and Instrumentation

According to the biomechanics and structural characteristics and the working principle of the exoskeleton, an experimental platform for spiral spring was designed. The experimental characterization of the torsional elastic module was conducted using a custom-made test rig. The test rig comprises a grounded base, spiral spring, pully, ball bearing, and cable, as shown in Figure 16. The parts of the test reg were chosen to be effective and low-cost within the simplified configuration.

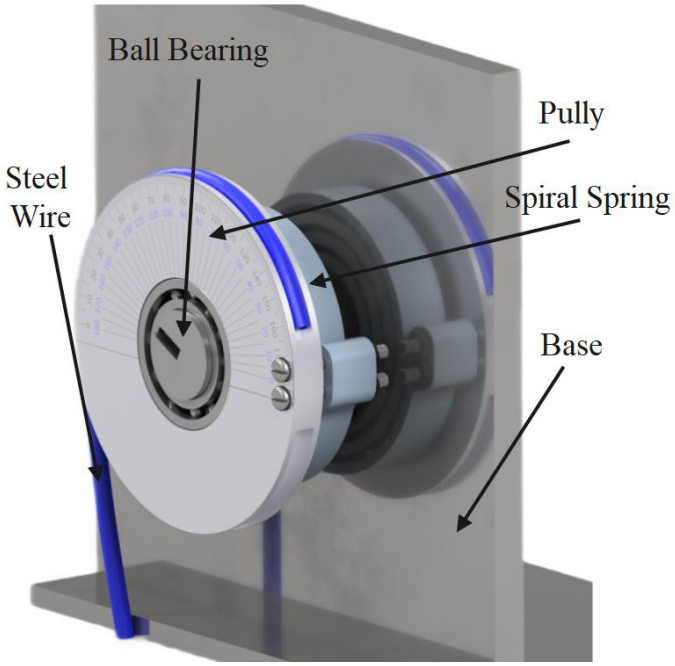

Figure 16. 3D rendering of the test reg.

The spiral spring, which is the side of the energy storage unit, was located in the ground of the experimental platform by its inner diameter, as shown in Figure 16, which represents how it connected to the cover case of the actuator body (ES-RSEA). The external diameter of the spiral spring was connected to the pulley transmission system by a bolt. This connection simulated the torque transmission from the input swing motion of the output link of the actuator, in which the rotary movement is transformed from the attached human thigh. Moreover, the wire rope is integrated and mounted to the pulley to apply a known torque to the spiral spring by hanging a known mass on the other side of the cable. The deflection angle of a spiral spring can be counted by a protractor, which is

Preprints (www.preprints.org) | NOT PEER-REVIEWED | Posted: 14 June 2022 doi:10.20944/preprints202206.0200.v1

a traditional and low-cost gadget for angle measurement. Since the applied torque and deflection angle are not in a fluctuation or dynamic pattern, the protractor would be sufficient to measure the deflection angle instead of using an expensive encoder sensor. Figure 16 shows the spiral spring placed on the testbed in the unloaded condition. The load is applied through a steel wire (Figure 16, 304 stainless steel wire rope, diameter 1.2 mm) connected to the moving pulley (Figure 16, radius 45 mm). The resulting torque was transmitted to the outer ring of the spring, while the inner ring was fixed to the frame (Figure 16, diameter 25 mm). The angular deflection was measured by a protractor placed on the pully.

6. Results and Discussion

6.1. Results

In the experiment, the spiral spring prototype was thus characterized by implementing the progressive value of torque from 1.1 N.m to 20.9 Nm with increments of 1.1 Nm. These values relate to masses suspended by steel wire ranging from 2.5 kg to 47.5 kg, increasing at 2.5 kg increments. The spiral spring was tested three times to eliminate random error, so each applied torque was repeated three times to enable the spring to return to its original position after each measurement; the three measured tests and the average values are shown in Figure 17**Error! Reference source not found.**. The real-time data will be recorded manually and then derived from the data by making the curves of the assisting torque and angle, as shown in Figure 17.

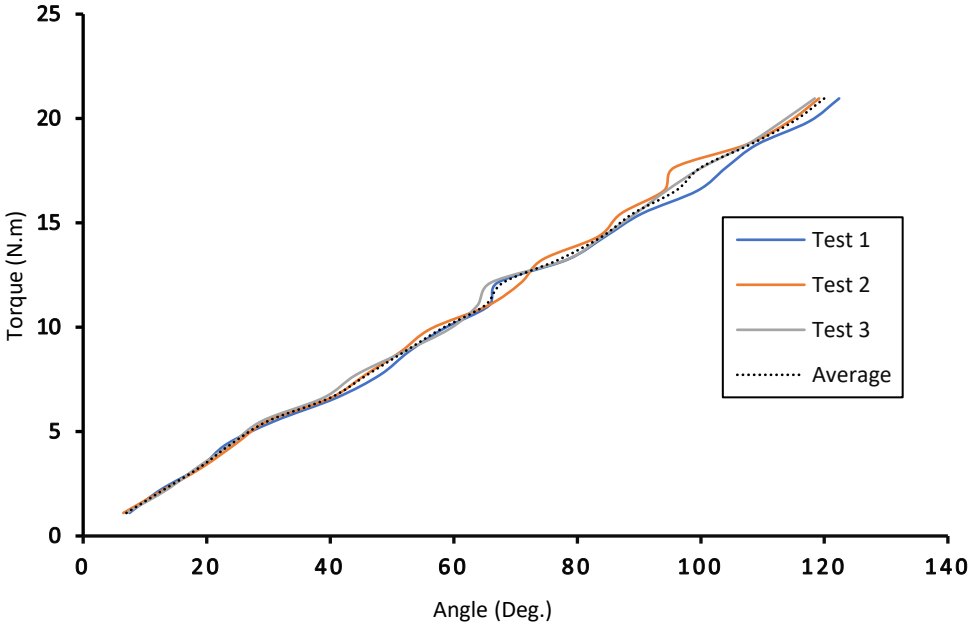

Figure 17. Characteristic of spiral spring stiffness for three tests.

Preprints (www.preprints.org) | NOT PEER-REVIEWED | Posted: 14 June 2022 doi:10.20944/preprints202206.0200.v1

The torque versus rotation characteristics of the experimental average values and theoretical spiral spring modules are shown in Figure 18

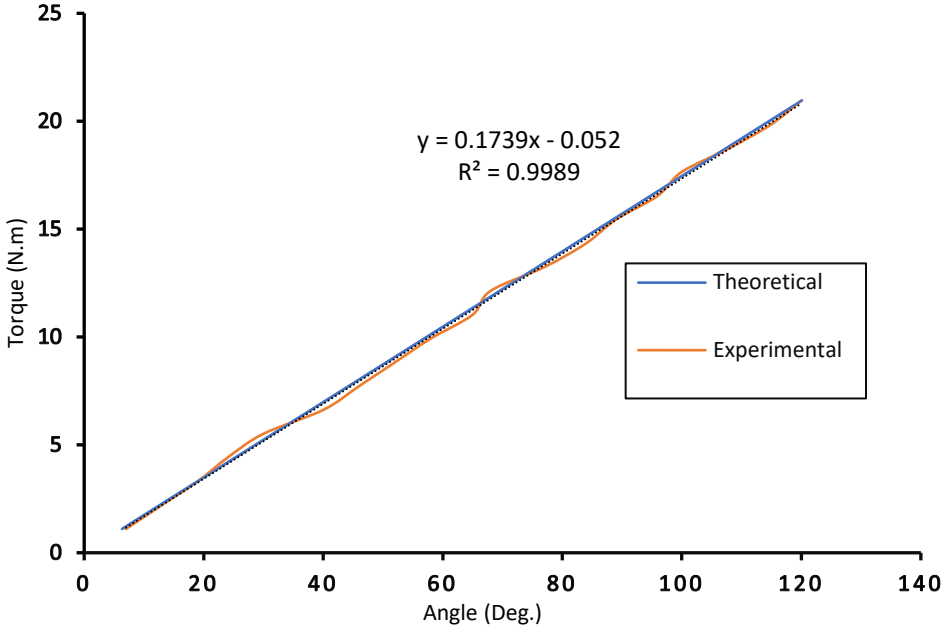

Figure **Error! Reference source not found.**. As noted, the corresponding residuals and the results of a linear regression fit were collected for the rotation of the pully and outer ring of the spiral spring. The dotted line represents linear regression (R^2 = 0.9989) for data collected during the experimental test. On the same plot, theoretical data are introduced using a linear regression displayed by the solid line (R^2 = 1.000) Theoretical calculations predicted a stiffness $k_{th.}$ = 10 Nm/rad, but experimental measurements showed $k_{exp.}$= 9.96 Nm/rad stiffness, resulting in a 0.36 percent difference between theoretical and experimented data, calculated as $(k_{exp.} - k_{th.})/k_{th.}$. In addition, the spring has maximum stored energy reaching 21.85 J when 20.9 Nm torque is applied and reaches the maximum deflection of 120 degrees, based on the experimentally measured stiffness characteristics, as shown in Figure 19.

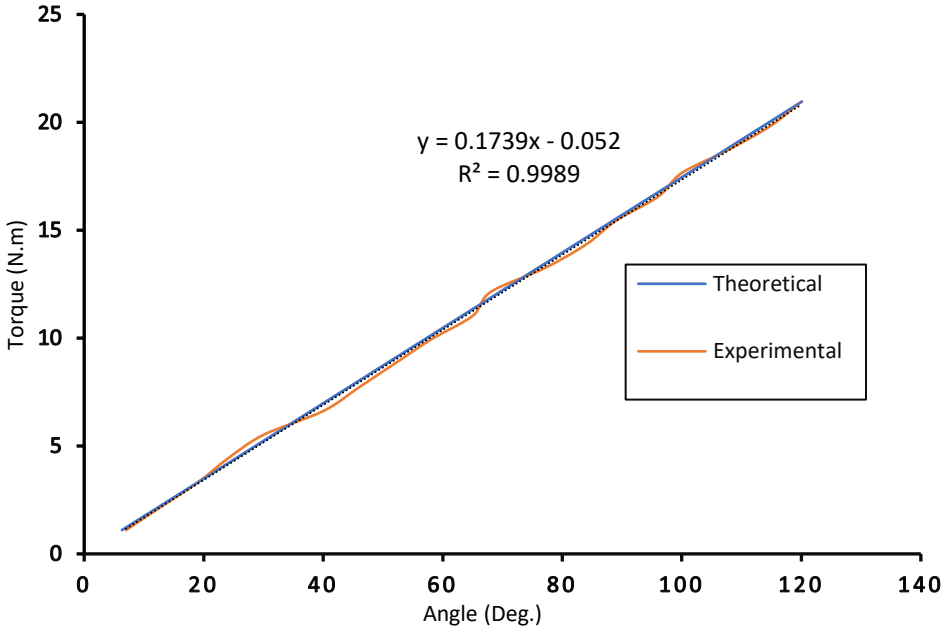

Preprints (www.preprints.org) | NOT PEER-REVIEWED | Posted: 14 June 2022 doi:10.20944/preprints202206.0200.v1

Figure 18. Characteristic of spiral spring stiffness the average experimental values and theoretical curves.

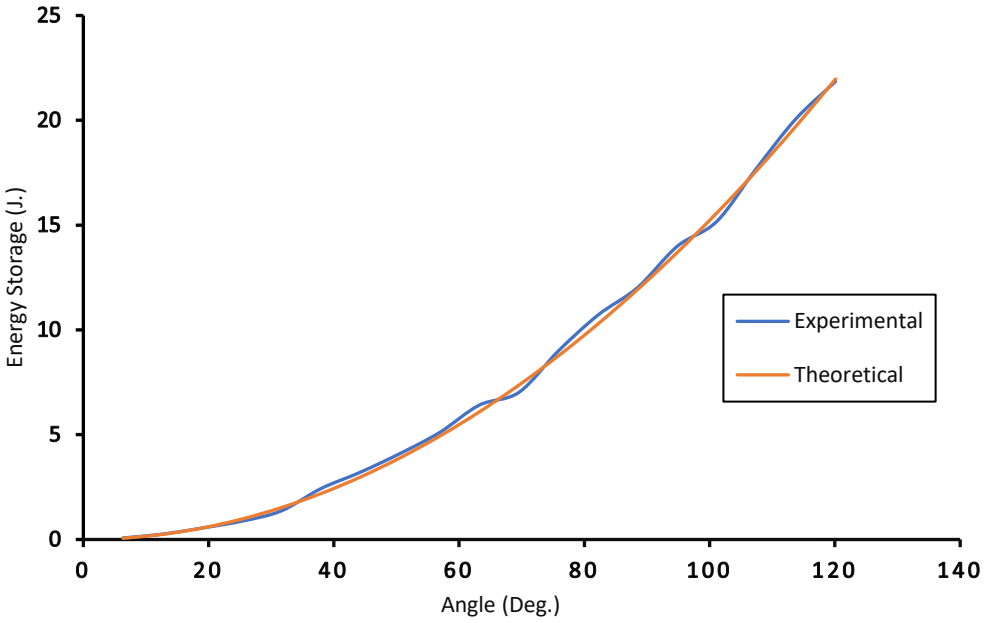

Figure 19. Energy storage Characteristic of spiral spring

The results showed that the entire design of ES-RSEA for the lumbar support exoskeleton provides the maximum output torque assistance, reaching 20.9 Nm during the descent phase and 66.6 Nm during the ascent phase, as shown in Table 4. During the ascent phase, the overall output torque is combined with the DC motor's peak output torque (45.7 Nm) and the output torque of the stored energy device (20.9 Nm). The DC motor is only turned on during the ascent phase, while it is turned off in the descent phase. However, this proposed strategy is advantageous in term of increasing the battery life and reducing battery size because it satisfies the function of the motor in a single stage.

Table 4. Compression of maximum output torque assistance for lumbar support exoskeletons

Lumbar support exoskeleton design	Maximum continuous output torque	
	Descent phase / DC motor (ON/OFF)	Ascent phase/ DC motor (ON/OFF)
ES-RSEA (proposed design)	20.9 Nm / OFF	66.6 Nm / ON
Robo-Mate/PEA (Mk2) [53]	28.9 Nm / ON	28.9 Nm/ ON
Waist Assist Exoskeleton [18]	64 Nm / ON	64 Nm / ON
Powered Hip Exoskeleton/ SEA [24]	40 Nm / ON	40 Nm / ON
H-WEXv2/ SEA [25]	90 Nm / ON	90 Nm / ON
HAL [54]	15 Nm / ON	15 Nm / ON
Stand-alone powered exoskeleton robot suit [55]	57 Nm / ON	57 Nm / ON

6.2. Discussion

The findings of this study have revealed the efficiency and robustness of the design of a compact energy storage with a rotary series elastic actuator for lumbar support

 doi:10.20944/preprints202206.0200.v1

exoskeleton. Considering the design, the experimental version of the storage device prototype is used to verify the design concept, transmission, and storage principle. The applied output torque in the experiment test represents the maximum output torque capacity that a spiral spring can withstand. Also, the angular deflection measured on the spiral spring prototype represents the range of motion that the human body can experience during the actual lifting tasks.

The experiment results of energy storage show almost identical curve with the theoretical outputs. The lumbar support exoskeleton can accomplish more extensive output capacities with stored energy based on the movements of the workers during lifting tasks with a wide range of hip angles provided the proper spiral spring is used. The energy release is not executed instantaneously because the exoskeleton releases the energy gradually with the help of the deformation of the spiral spring. After the gear drive (harmonic drive), the output link is driven to rotate, and the power is rapidly increased, which is associated with the movement of the hip angle during the decent stage. Subsequently, the elastic potential energy gradually decreases with the recovery of spiral spring deformation during the ascent stage.

The results of biomechanics of the human lower limbs show that the characteristics of the spiral spring can be efficiently featured as a central part of the proposed storage device. Based on the biomechanics of the human lower limbs, the human kinematics and kinetics data from the literature [36] indicate appropriate support and provide power and load assistance for the lumbar spine during the lifting task, combined with the physiological structure of the hip joint. In line with this, the results obtained from ES-RSEA show the lumbar support exoskeleton provided the maximum assisting torque during both the descent and ascent phases.

The spiral springs is designed and optimized to reduce both weight and size while maintaining the required spring stiffness and spring deformation. The test indicate that the spiral spring constantly try to return to its original shape because of its stiffness; it can generate the opposite torque to gravity, resulting in the minimum torque required for the hip joint. It is designed to absorb and store the biomechanical energy distributed at the hip joints during the descent phase of a squatting cycle and then release it in the ascent phase. However, the characteristic curve of a spiral spring is greatly affected by the number of coils. With the increase in the number of turns, the characteristic curve is more and more inclined toward the straight line. Combined with theoretical analysis, the bending moment of the spiral spring is proportional to the rotation angle, which is reflected as an oblique line with constant slope. But the real characteristic curve is not an ideal oblique line. After the spring is subjected to external force, the rotation and bending deformation of the spring cannot be accurately predicted. This is because the designed spiral spring's primary behavior is the linear characteristic curve since the spring is coiled firmly, where each coil of the spring is strained when the external torque is applied. Once the inner coil and outer coil revolve relative to each other, the flexible element will cause elastic deformation to guarantee the torque transfer and mitigate the impact. Therefore, the flexible element acts as a bridge to transmit the applied torque between the coils. In support of this finding, [49] employed a unidirectional series-elastic actuator design for spiral torsion spring showed precise estimate of bending deformation of the spring not achievable.

Moreover, the friction and extrusion between the coils of the spiral spring affect the normal operation. After many experiments and comparative analysis, we found that there is a certain deviation between the experimental value and the theoretical value, which is caused by a factor, such as external force. There must be friction in the experiment, which will affect the experimental accuracy. Friction breaks the balance of the original force system and is inevitably affected by external forces, resulting in the change of the bending characteristic curve. Spiral springs, as a result, have a linear torque-deflection relation.

The results of the torque-deflection angle relationship showed that the stiffness characteristics response is quite linear under the tested torque range, representing over 99% linearity. Additionally, there is no significant hysteresis. The stiffness values vary by less than 1%, depending on the loading direction estimated by the experimental and

 doi:10.20944/preprints202206.0200.v1

theoretical results. Therefore, the spring stiffness is relatively uniform. Therefore, the spring deformation is stable and symmetric, as the curve plot illustrates. However, the difference between the experimental and simulated results is less than 2%, which is considered an insignificant difference.

Compared with other lumbar support exoskeletons, the ES-RSEA has yielded encouraging results that exceed the level of other exoskeletons' assistance in the literature [49]. The comparison is limited to research that used actuators with DC motors in order to provide a fair comparison. The findings reveal that the ES-RSEA lumbar support exoskeleton's entire design delivers maximal output torque assistance throughout the ascent phase. The overall output torque is coupled with the peak output torque of the DC motor and the output torque of the stored energy device during the ascent phase. In addition, the proposed strategy is advantageous in terms of improving the battery life and battery size since it fulfills the motor's purpose in a single stage. In other words, the performance and operation setting of the spiral spring and DC motor determine the lifting strategy during the ascent phase of the semi squat cycle. However, each phase employs a different function strategy between active and passive actuation of the DC motor and spiral spring, respectively. The maximum assistive torque occurs in the ascent phase, where the output torque results from a combination of the DC motor's torque and the released torque of the spiral spring. Furthermore, the DC motor is powered and runs in the same direction as human movement to exert positive work. In the same direction, the spiral spring starts to release its stored energy and torque during the ascent phase. Since the released torque of the spiral spring and the SEA output torque are oriented toward the same direction, there is no energy loss between the output of the SEA and the spring.

7. Conclusion and Suggestions for Future Work

This article offers a supplement lifting solution for workers to improve their lifting abilities while performing manual lifting handling tasks. The structural design and prototype machining test of the spiral spring have been established and tested. The results revealed that the stiffness of the spiral spring is quite uniform and linear with significant storage energy. The ES-RSEA for the lumbar support exoskeleton has generated assistive output torque in both descent and ascent phases. The RSEA provided mechanical compliance with output torque at the interface between the exoskeleton and the user. At the same time, an energy storage (ES) unit utilized the negative work of lower limbs and satisfied the need for the external energy during the descent phase. The characteristics of the spiral spring has been efficiently featured as the primary element of energy storage unit, and it plays a vital role in providing additional torque to the overall actuator output. This spiral spring stored mechanical energy when the wearer bends forward and lowers the body to lift the load, where the kinetic energy of the lower limb was converted into potential energy. Subsequently, this stored energy in the mechanical spring can be released at the start of lifting an object to assist the acceleration motion as assistance torque alongside with the RSEA output torque.

The lumbar support exoskeleton consists of a flexible mechanical structure with a compact modular rotary series elastic actuator integrated with an energy storage device. The entire ES-RSEA design transformed energy in lifting activities without interfering with the natural movement of the lumbar spine. A passive energy storage device (ES) stores and discharges energy supplied by humans because of the physical components employed. The mechanical storage device has higher energy, participates in energy management, and can provide unilateral lower limb assistance for the workers during the manual lifting handling tasks to achieve energy migration and improve autonomous mobility. Simultaneously, the active rotary series elastic actuator (RSEA) provides extra energy from external sources (e.g., batteries) on request. The spiral spring has been chosen as the energy storage device because it is reusable, low cost, pollution-free, exploiting the privileges of the hip joint movement. The design of the spiral spring displayed excellent performance. Spiral springs collaborate with SEA to give high torque support for lifting tasks, as demonstrated by the lifting strategy and energy conversion of biomechanical

 doi:10.20944/preprints202206.0200.v1

energy based on storing and releasing during the semi-squat lifting cycle. Therefore, the key contributions of the proposed design include

i) It provides physical support for the daily lifting tasks for workers so that the wearer can complete their lifting tasks without risking a lower back injury.

ii) The designed actuation system provides excellent compliance and flexibility, preventing any injury from the human body's undesired movement and reducing exoskeleton structure and motor damage.

iii) The designed realize the energy storage of human energy, exploit the biomechanics of lifting tasks, and mitigate the burden of human effort to perform this task.

iv) Reduce the battery consumption rate and working hours for the DC motor.

The overall results indicate potential advantages of the proposed ES-RSEA actuator for lumbar support exoskeleton. The future research needs to focus on the following challenges: (a) Because of its energy-storing feature for lifting tasks, ES-RSEA can serve as a critical criterion in providing higher lifting assistance, reducing muscle activity and metabolic consumption. (b) Wearing an exoskeleton integrated with ES-RSEA and measuring human performance (e.g., kinetics and electromyography) might be a future emphasis. (c) however, SEA control methods will need to be investigated to increase the performance of SEA since the series elastic actuator consists of spring elements to provide compliance. (d) Because the value of the human side parameters varies with joint angles, a robust torque controller is required to enable optimal torque monitoring independent of the joint angle value. Finally, (e) high-efficiency energy storage rotary series elastic actuator (ES-RSEA) is expected to be developed with improved follow-up research effort.

 doi:10.20944/preprints202206.0200.v1

Author Contributions: Conceptualization, O.A.; methodology, O.A.; software, O.A. ; validation, O.A., R.G., M.T., and H.Y.; formal analysis, O.A.; investigation, O.A.; resources, R.G., and H.Y.; data curation, O.A.; writing—original draft preparation, O.A.; writing—review and editing, O.A, M.T., R.G., and E.A.; visualization, O.A., R.G., M.T., and H.Y.; supervision, R.G., H.Y., and M.T.; project administration, R.G., and H.Y.; funding acquisition, O.A, R.G. M.T., H.Y. and E.A. .All authors have read and agreed to the published version of the manuscript.

Funding: The project has been supported with provision of facility and equipment by University of Malaya under faculty of engineering Grant (GPF023A-2018).

Data Availability Statement: All the relevant data are within the paper and its supporting information files

Acknowledgments: The authors wish to acknowledge the support by University of Malaya for the facility and equipment support under faculty of engineering Grant (GPF023A-2018).

Conflicts of Interest: The authors declare no conflict of interest. The funders had no role in the design of the study; in the collection, analyses, or interpretation of data; in the writing of the manuscript, or in the decision to publish the results.

References

1. Kazerooni, H. Human power amplifier for lifting load including apparatus for preventing slack in lifting cable. 24 November 2000 2000.
2. de Looze, M.P.; Bosch, T.; Krause, F.; Stadler, K.S.; O'Sullivan, L.W. Exoskeletons for industrial application and their potential effects on physical work load. *Ergonomics* **2016**, *59*, 671-681, doi:10.1080/00140139.2015.1081988.
3. Yang, Z.; Gu, W.; Zhang, J.; Gui, L. *Force control theory and method of human load carrying exoskeleton suit*; Springer: 2017.
4. Young, A.J.; Ferris, D.P. State of the Art and Future Directions for Lower Limb Robotic Exoskeletons. *IEEE Trans Neural Syst Rehabil Eng* **2017**, *25*, 171-182, doi:10.1109/TNSRE.2016.2521160.
5. Ko, H.K.; Lee, S.W.; Koo, D.H.; Lee, I.; Hyun, D.J. Waist-assistive exoskeleton powered by a singular actuation mechanism for prevention of back-injury. *Robotics and Autonomous Systems* **2018**, *107*, 1-9, doi:10.1016/j.robot.2018.05.008.
6. Wehner, M.; Rempel, D.; Kazerooni, H. Lower Extremity Exoskeleton Reduces Back Forces in Lifting. In Proceedings of the ASME 2009 Dynamic Systems and Control Conference, 2009; pp. 49-56.
7. Baltrusch, S.J.; van Dieën, J.H.; Koopman, A.S.; Näf, M.B.; Rodriguez-Guerrero, C.; Babič, J.; Houdijk, H. SPEXOR passive spinal exoskeleton decreases metabolic cost during symmetric repetitive lifting. *European Journal of Applied Physiology* **2020**, *120*, 401-412, doi:10.1007/s00421-019-04284-6.
8. Ulrey, B.L.; Fathallah, F.A. Subject-specific, whole-body models of the stooped posture with a personal weight transfer device. *Journal of Electromyography and Kinesiology* **2013**, *23*, 206-215, doi:10.1016/j.jelekin.2012.08.016.
9. Näf, M.B.; Koopman, A.S.; Baltrusch, S.; Rodriguez-Guerrero, C.; Vanderborght, B.; Lefeber, D. Passive Back Support Exoskeleton Improves Range of Motion Using Flexible Beams. *Frontiers in Robotics and AI* **2018**, *5*, doi:10.3389/frobt.2018.00072.
10. Kazerooni, H.; Tung, W.; Pillai, M. Evaluation of Trunk-Supporting Exoskeleton. *Proceedings of the Human Factors and Ergonomics Society Annual Meeting* **2019**, *63*, 1080-1083, doi:10.1177/1071181319631261.
11. Frost, D.M.; Abdoli, E.M.; Stevenson, J.M. PLAD (personal lift assistive device) stiffness affects the lumbar flexion/extension moment and the posterior chain EMG during symmetrical lifting tasks. *Journal of Electromyography and Kinesiology* **2009**, *19*, e403-412, doi:10.1016/j.jelekin.2008.12.002.
12. Imamura, Y.; Tanaka, T.; Suzuki, Y.; Takizawa, K.; Yamanaka, M. Motion-based design of elastic belts for passive assistive device using musculoskeletal model. In Proceedings of the 2011 IEEE International Conference on Robotics and Biomimetics, 7-11 Dec. 2011, 2011; pp. 1343-1348.
13. Heydari, H.; Hoviattalab, M.; Azghani, M.R.; Ramezanzadehkoldeh, M.; Parnianpour, M. INVESTIGATION ON A DEVELOPED WEARABLE ASSISTIVE DEVICE (WAD) IN REDUCTION LUMBAR MUSCLES ACTIVITY. *Biomedical Engineering: Applications, Basis and Communications* **2013**, *25*, 1350035, doi:10.4015/s101623721350035x.
14. Lamers, E.P.; Yang, A.J.; Zelik, K.E. Feasibility of a Biomechanically-Assistive Garment to Reduce Low Back Loading During Leaning and Lifting. *IEEE Trans. Biomed. Eng.* **2018**, *65*, 1674-1680, doi:10.1109/TBME.2017.2761455.
15. Alemi, M.M.; Geissinger, J.; Simon, A.A.; Chang, S.E.; Asbeck, A.T. A passive exoskeleton reduces peak and mean EMG during symmetric and asymmetric lifting. *Journal of Electromyography and Kinesiology* **2019**, *47*, 25-34, doi:10.1016/j.jelekin.2019.05.003.
16. Ji, X.; Wang, D.; Li, P.; Zheng, L.; Sun, J.; Wu, X.; Yang, Z. SIAT-WEXv2: A Wearable Exoskeleton for Reducing Lumbar Load during Lifting Tasks. *Complexity* **2020**, *2020*, 1-12, doi:10.1155/2020/8849427.
17. Gopura, R.A.R.C.; Kiguchi, K.; Bandara, D.S.V. A brief review on upper extremity robotic exoskeleton systems. In Proceedings of the 2011 6th International Conference on Industrial and Information Systems, 16-19 Aug. 2011, 2011; pp. 346-351.
18. Yong, X.; Yan, Z.; Wang, C.; Wang, C.; Li, N.; Wu, X. Ergonomic Mechanical Design and Assessment of a Waist Assist Exoskeleton for Reducing Lumbar Loads During Lifting Task. *Micromachines (Basel)* **2019**, *10*, 463, doi:10.3390/mi10070463.

19. von Glinski, A.; Yilmaz, E.; Mrotzek, S.; Marek, E.; Jettkant, B.; Brinkemper, A.; Fisahn, C.; Schildhauer, T.A.; Gessmann, J. Effectiveness of an on-body lifting aid (HAL(R) for care support) to reduce lower back muscle activity during repetitive lifting tasks. *the Journal of Clinical Neuroscience* **2019**, *63*, 249-255, doi:10.1016/j.jocn.2019.01.038.
20. ATOUN Inc. Available online: http://atoun.co.jp/ (accessed on
21. Ito, T.; Ayusawa, K.; Yoshida, E.; Kobayashi, H. Stationary torque replacement for evaluation of active assistive devices using humanoid. In Proceedings of the 2016 IEEE-RAS 16th International Conference on Humanoid Robots (Humanoids), 15-17 Nov. 2016, 2016; pp. 739-744.
22. Pratt, G.A.; M. Williamson, M. Series elastic actuators. In Proceedings of the Proceedings 1995 IEEE/RSJ International Conference on Intelligent Robots and Systems. Human Robot Interaction and Cooperative Robots, 1995; pp. 399-406 vol.391.
23. Toxiri, S.; Koopman, A.S.; Lazzaroni, M.; Ortiz, J.; Power, V.; de Looze, M.P.; O'Sullivan, L.; Caldwell, D.G. Rationale, Implementation and Evaluation of Assistive Strategies for an Active Back-Support Exoskeleton. *Frontiers in Robotics and AI* **2018**, *5*, 53, doi:10.3389/frobt.2018.00053.
24. Zhang, T.; Huang, H. A Lower-Back Robotic Exoskeleton: Industrial Handling Augmentation Used to Provide Spinal Support. *IEEE Robotics & Automation Magazine* **2018**, *25*, 95-106, doi:10.1109/mra.2018.2815083.
25. Hyun, D.J.; Lim, H.; Park, S.; Nam, S. Singular Wire-Driven Series Elastic Actuation with Force Control for a Waist Assistive Exoskeleton, H-WEXv2. *IEEE/ASME Transactions on Mechatronics* **2020**, *25*, 1026-1035, doi:10.1109/tmech.2020.2970448.
26. Chaichaowarat, R.; Kinugawa, J.; Kosuge, K. Unpowered Knee Exoskeleton Reduces Quadriceps Activity during Cycling. *Engineering* **2018**, *4*, 471-478, doi:https://doi.org/10.1016/j.eng.2018.07.011.
27. Robertson, D.G.; Wilson, J.M.; St Pierre, T.A. Lower extremity muscle functions during full squats. *Journal of Applied Biomechanics* **2008**, *24*, 333-339, doi:10.1123/jab.24.4.333.
28. Vecchio, L.D. Choosing a Lifting Posture: Squat, Semi-Squat or Stoop. *MOJ Yoga & Physical Therapy* **2017**, *2*, doi:10.15406/mojypt.2017.02.00019.
29. Paradiso, J.A.; Starner, T. Energy Scavenging for Mobile and Wireless Electronics. *IEEE Pervasive Computing* **2005**, *4*, 18-27, doi:10.1109/mprv.2005.9.
30. Zhou, X.; Liu, G.; Han, B.; Wu, L.; Li, H. Design of a Human Lower Limbs Exoskeleton for Biomechanical Energy Harvesting and Assist Walking. *Energy Technology* **2020**, *9*, 2000726, doi:10.1002/ente.202000726.
31. Penrose, D. *Occupational Therapy for Orthopaedic Conditions*; Springer US: 2013.
32. Byrne, D.P.; Mulhall, K.J.; Baker, J.F. Anatomy & biomechanics of the hip. *The open sports medicine Journal* **2010**, *4*.
33. Ricciardi, A. Thieme Atlas of Anatomy: General Anatomy and Musculoskeletal System. *Yale J Biol Med* **2015**, *88*, 100.
34. Mann, G.K.I.; Jayawardena, T.S.S.; Gopura, R.A.R.C.; Ranaweera, R.K.P.S. Development of A Passively Powered Knee Exoskeleton for Squat Lifting. *Journal of Robotics, Networking and Artificial Life* **2018**, *5*, 45-51, doi:10.2991/jrnal.2018.5.1.11.
35. Toxiri, S.; Ortiz, J.; Masood, J.; Fernández, J.; Mateos, L.A.; Caldwell, D.G. A wearable device for reducing spinal loads during lifting tasks: Biomechanics and design concepts. In Proceedings of the 2015 IEEE International Conference on Robotics and Biomimetics (ROBIO), 6-9 Dec. 2015, 2015; pp. 2295-2300.
36. Masood, J.; Ortiz, J.; Fernandez, J.; Mateos, L.A.; Caldwell, D.G.; Ieee. Mechanical Design and Analysis of Light Weight Hip Joint Parallel Elastic Actuator for Industrial Exoskeleton. In Proceedings of the 2016 6th Ieee International Conference on Biomedical Robotics and Biomechatronics, New York, 2016; pp. 631-636.
37. Cenciarini, M.; Dollar, A.M. Biomechanical considerations in the design of lower limb exoskeletons. In Proceedings of the IEEE International Conference on Rehabilitation Robotics, 2011; p. 5975366.
38. Winter, D.A. *Biomechanics and motor control of human movement*; John Wiley & Sons: 2009.
39. Low, K.H.; Xiaopeng, L.; Haoyong, Y. Development of NTU wearable exoskeleton system for assistive technologies. In Proceedings of the IEEE International Conference Mechatronics and Automation, 2005, 29 July-1 Aug. 2005, 2005; pp. 1099-1106 Vol. 1092.

40. Aguilar-Sierra, H.; Yu, W.; Salazar, S.; Lopez, R. Design and control of hybrid actuation lower limb exoskeleton. *Advances in Mechanical Engineering* **2015**, *7*, doi:10.1177/1687814015590988.
41. Hassan, s.N.; Yusuff, R.; Md Zein, R.; Hussain, R.; Tamil Selvan, H.K. *Anthropometric data of Malaysian workers*; 2015; pp. 353-360.
42. Minchala, L.I.; Astudillo - Salinas, F.; Palacio - Baus, K.; Vazquez - Rodas, A. Mechatronic Design of a Lower Limb Exoskeleton. In *Design, Control and Applications of Mechatronic Systems in Engineering*; 2017.
43. Carpino, G.; Accoto, D.; Sergi, F.; Luigi Tagliamonte, N.; Guglielmelli, E. A Novel Compact Torsional Spring for Series Elastic Actuators for Assistive Wearable Robots. *Journal of Mechanical Design* **2012**, *134*, 121002-121002-121010, doi:10.1115/1.4007695.
44. W. Robinson, D. Design and Analysis of Series Elasticity in Closed-loop Actuator Force Control. Doctoral dissertation Massachusetts Institute of Technology, 2000.
45. Tagliamonte, N.L.; Sergi, F.; Carpino, G.; Accoto, D.; Guglielmelli, E.; Ieee. Design of a Variable Impedance Differential Actuator for Wearable Robotics Applications. In Proceedings of the Ieee/Rsj 2010 International Conference on Intelligent Robots and Systems, Taipei, Taiwan, 2010; pp. 2639-2644.
46. J, Y. Control method and experimental research on elastic actuation of exoskeleton robot. Master's thesis Harbin Institute of Technology, 2014.
47. Robinson, D.W.; Pratt, J.E.; Paluska, D.J.; Pratt, G.A. Series elastic actuator development for a biomimetic walking robot. In Proceedings of the 1999 IEEE/ASME International Conference on Advanced Intelligent Mechatronics (Cat. No.99TH8399), 19-23 Sept. 1999, 1999; pp. 561-568.
48. Lee, C.; Kwak, S.; Kwak, J.; Oh, S. Generalization of Series Elastic Actuator Configurations and Dynamic Behavior Comparison. *Actuators* **2017**, *6*, 26.
49. Knox, B.T.; Schmiedeler, J.P. A Unidirectional Series-Elastic Actuator Design Using a Spiral Torsion Spring. *Journal of Mechanical Design* **2009**, *131*, 125001-125001-125005, doi:10.1115/1.4000252.
50. Associated, S. *Engineering Guide to Spring Design*, 2021 ed.; Associated Spring, Barnes Group Inc.: 44330 Plymouth Oaks Blvd Plymouth, MI 48170, 1987.
51. Bensky, T.J. Energy: kinetic, potential, conservation, and work. *Exploring Physics with Computer Animation and PhysGL* **2016**, 10-11-10-19, doi:10.1088/978-1-6817-4425-4ch10.
52. Inc., C.M. 4 Features That Make Waterjet Cutting the Right Choice for Your next Metal Fabrication Project. Available online: https://inbound.cammmetals.com/blog/4-features-that-make-waterjet-cutting-the-right-choice-for-your-next-metal-fabrication-projec (accessed on 29 Oct. 2018).